



HAL
open science

A new miniature magnetometer based on a quartz MEMS Resonator and a Stack of Magnetic Materials

Charles Mauc, Thomas Perrier, Raphael Levy, Johan Moulin

► To cite this version:

Charles Mauc, Thomas Perrier, Raphael Levy, Johan Moulin. A new miniature magnetometer based on a quartz MEMS Resonator and a Stack of Magnetic Materials. IEEE 35th International Conference on Micro Electro Mechanical Systems Conference (MEMS 2022), IEEE, Jan 2022, Tokyo, Japan. pp.955-958, 10.1109/MEMS51670.2022.9699574 . hal-04102763

HAL Id: hal-04102763

<https://hal.science/hal-04102763>

Submitted on 22 May 2023

HAL is a multi-disciplinary open access archive for the deposit and dissemination of scientific research documents, whether they are published or not. The documents may come from teaching and research institutions in France or abroad, or from public or private research centers.

L'archive ouverte pluridisciplinaire **HAL**, est destinée au dépôt et à la diffusion de documents scientifiques de niveau recherche, publiés ou non, émanant des établissements d'enseignement et de recherche français ou étrangers, des laboratoires publics ou privés.

A NEW MINIATURE MAGNETOMETER BASED ON A QUARTZ MEMS RESONATOR AND A STACK OF MAGNETIC MATERIALS

Charles D. Mauc^{1,2}, Thomas Perrier¹, Raphaël Levy¹ and Johan Moulin²

¹ONERA, the French Aerospace Lab, Avenue de la division Leclerc, Châtillon, France

²C2N, Boulevard Thomas Gaubert, Palaiseau, France

ABSTRACT

This paper presents an innovative 1D MEMS resonating magnetometer exploiting the torque induced by the external magnetic field on a stack of ferromagnetic and antiferromagnetic materials. It is targeted for applications such as magneto-inertial navigation. The sensor was successfully fabricated using a wet chemical process and its working principle was proven correct. The experimental results showed a sensitivity of 1500 Hz/T and an estimated resolution of 7.3 nT.

KEYWORDS

Magnetometer, MEMS, quartz, DETF, exchange bias

INTRODUCTION

Applications like magneto-inertial navigation [1] or the correction of the gyroscopes bias rely on magnetometers able to measure the spatial variations of the surrounding magnetic field. They are expected to be embedded and have a resolution below 10 nT over $[-1 \text{ mT}; 1 \text{ mT}]$.

Several types of magnetic sensors such as Hall sensors, fluxgates, AMR and MEMS magnetometers can be embedded. Among those last, most of them use as their core mechanism the Lorentz force [2], [3] Bian *et al* takes advantage of the magnetostriction [4] and finally some exploit the torque induced by the external magnetic field on a ferromagnetic thin film [5]. They can either have a frequency or voltage output combined with a capacitive or frequency shift or piezoresistive sensing.

The purpose of this paper is to present a new concept of high-resolution MEMS magnetometer. We will introduce the working principle as well as the choices of design for the resonator, the fabrication process and the experimental measurements of the sensitivity to the magnetic field.

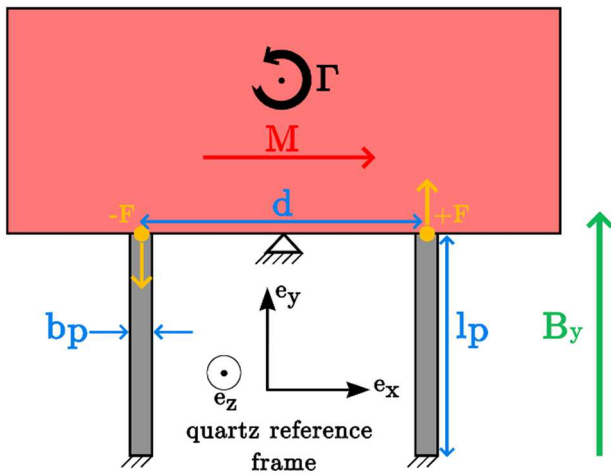


Figure 1. Working principle of the resonator

WORKING PRINCIPLE

The resonator is made out an α -quartz Z-cut wafer and is composed of several parts: two identical beams vibrating in flexural mode used as a differential force sensor, the pivot and a plate where the magnetic materials are deposited on (Figure 1). Those last are supposed to have a homogenous magnetization in one direction such as $\vec{M} = M \cdot \vec{e}_x$.

When there is no surrounding magnetic field the beams vibrate at the same resonance frequency: $f_1 = f_2$. However, when $\vec{B}_{ext} \neq \vec{0}$, the plate with the magnetic materials experiences a torque $\vec{\Gamma}$ which bend the structure. It depends on the volume of ferromagnetic material V_{magn} and \vec{B}_{ext} :

$$\vec{\Gamma} = M \cdot V_{magn} \cdot (B_y \cdot \vec{e}_z - B_z \cdot \vec{e}_y) = \vec{\Gamma}_{B_y} + \vec{\Gamma}_{B_z} \quad (1)$$

By design, the plate cannot turn around the pivot and not its gravity centre. On one hand, the $\vec{\Gamma}_{B_y}$ contribution compress one beam and stretch the other one within the (XY) plan, leading to an opposite frequency shift. On the other hand, the $\vec{\Gamma}_{B_z}$ contribution makes both beams bend out of the (XY) plan in a way that leads to the same frequency shift. This is why we can only take into account the $\vec{\Gamma}_{B_y}$ contribution which leads to the difference of resonance frequencies Δf :

$$\Delta f = f_1 - f_2 = K_B \cdot B_y \propto M \cdot V_{magn} \cdot \frac{1}{b_p^2 \cdot h_p} \cdot \frac{1}{d} \cdot B_y \quad (2)$$

Where K_B is the sensitivity, b_p is the cross-section ($\parallel \vec{e}_x$) and h_p is the thickness ($\parallel \vec{e}_z$) of the beam.

Another advantage of having two identical beams as a differential force sensor is the possibility to reduce a lot the influences of environmental perturbations such as acceleration, rotation and temperature. Indeed, such perturbations will shift the resonance frequencies of each beam the same way, which will lead to almost no shift of Δf .

DESIGN AND SIMULATION RESULTS

Choice of the wafer material

To make the beams vibrate into their flexural mode at low frequency, we chose to use the Z-cut α -quartz wafer. This material is piezoelectric so we can use electrodes to actuate the beams and the Z-cut is fitted for flexural mode at low frequency. Moreover, for such a beam, its resonance frequency will depends much less of the temperature than a beam made in another materials like silicon and the etch-rates in a chemical etching process are higher than other quartz cuts [6].

Differential force sensor geometry

The purpose of the finite elements simulation is to maximise the sensitivity to the B_y component of the external magnetic field, to maximise the quality factor Q and to minimise the resonance frequency f_R of the beams. Indeed, for frequency output sensors the detection limit depends on those parameters as such [7]:

$$\sigma(\tau) \propto \frac{f_R}{Q \cdot K_B} \quad (3)$$

Thanks to analytical model and the finite elements solver Oofelie::Multiphysics that was used within the scope of this study, an appropriate geometry for the force sensors was determined.

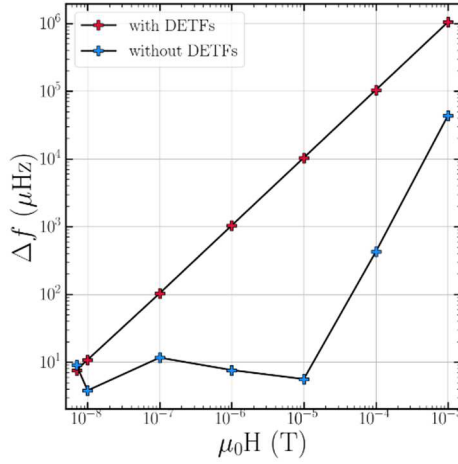


Figure 2. Simulated $\Delta f = f(B_y)$ for resonators with and without DETFs

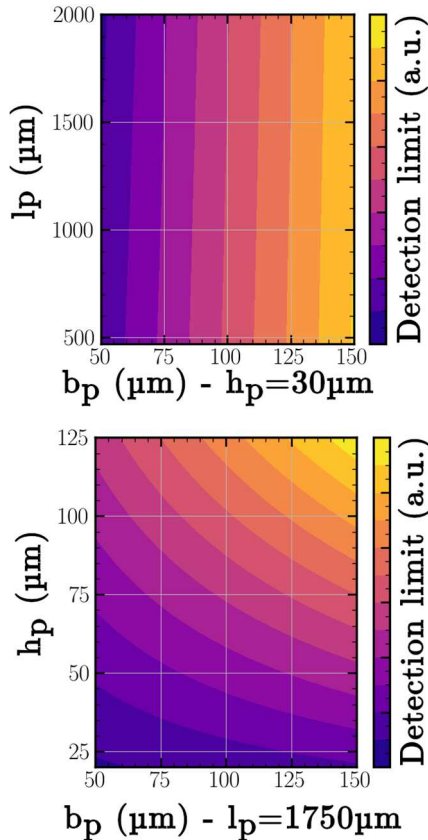


Figure 3. Detection limit as a function of b_p , l_p and h_p

When Δf is plotted as a function of B_y , the sensitivity of a resonator with simple beams is null for a magnetic field below 10^{-5} T when it is expected to be linear on the measurement scale. This is the result of the mechanical coupling between the two beams that tend to vibrate at the same frequency: the “lock-in” phenomenon (Figure 2) [8]. To prevent it to happen, it is possible to switch the simple beams for double-ended tuning forks (DETFs). In addition, in comparison with a simple beam, having a DETF allow to reduce greatly the anchor damping as a result of elastic waves destructive interferences due to the anti-phase vibratory mode of the two beams [9]. However, due to the doubling of the beams, the sensitivity K_B is divided by two.

The main contributions to the quality factor Q are the gas damping, anchor damping and thermoelastic dissipation (TED). Because the resonator will operate at $P = 1e^{-6}$ mBar leading to $Q_{gas} > 1e^6$ [10] and because a DETF has a simulated $Q_{anchor} > 1e^9$, it reasonable to assume that $Q \approx Q_{TED}$. Therefore, with an analytical model [11] it is possible to know which tendencies to follow when it comes to choose the dimensions of the beams: b_p , l_p and h_p . We can observe in the Figure 3 that the length of the beams has little to no influence on the detection limit; however, it is necessary to have the smallest cross-section b_p and thickness h_p to ensure the lowest detection limit. It is possible to ensure the mechanical robustness of the thin parts of the resonator with $h_p = 30 \mu\text{m}$. To secure the positioning and a sufficient width for the electrodes, we decided to have $b_p = 68 \mu\text{m}$.

Pivot

In order to reduce as much as possible the distance d between the DETFs, we chose not to align the pivot with the heads of the DETFs. Consequently, the sensitivity K_B increases a lot but the DETFs are not perfectly compressed or stretched along \vec{e}_y but also deformed along \vec{e}_x .

As location of the pivot, its design is a paramount importance for K_B . Unless the pivot is “virtual” i.e. geometrically constructed, the physical pivot of a MEMS cannot be perfect. To let the structure rotates more easily, we chose a pivot with branches (Figure 4) rather than a “filled” pivot (Figure 1).

Electrodes

The electrodes are meant to make the beams of the DETFs resonate thanks to the piezoelectric properties of the quartz. Because we want the beams to vibrate in flexural mode and because they are oriented toward the Y direction of the quartz, it is necessary to apply a positive electric field along the X direction on the parts of the beams being in tension and a negative electric field on the parts being in compression. To be consistent with the fabrication process, there are three electrodes placed on one side of the beams (Figure 4). Moreover, because we want the beams within one DETF to vibrate in anti-phase mode, the electrodes are symmetrically designed.

Magnetic materials

To have an homogeneous and stable magnetization M , we decided to take advantage of the exchange bias

appearing at the interface between an ferromagnetic and antiferromagnetic layer after an annealing procedure [12]. We chose a $\{\text{NiCr}(20\text{nm}) + [\text{NiMn}(50\text{nm}) + \text{CoFe}(50\text{nm})]^*10 + \text{NiMn}(50\text{nm})\}$ stack for its high magnetization and high exchange field [13].

EXPERIMENTAL RESULTS

Fabrication process of the resonator

The resonator was successfully fabricated thanks to a wet $\text{HF}/\text{NH}_4\text{F}$ etching of a $210\mu\text{m}$ thick quartz wafer (Figure 4). This process leads to the apparition of side-walls because the quartz has different etch-rates depending of its crystallographic orientation [6]. Their presence has a negative impact on the sensitivity to the magnetic field due to the increase of the cross-section of the beams. It also promotes a bad etching of the areas where there are many corners such as the heads of the DETFs (Figure 5). Moreover, the side-walls are not perfectly homogeneous so the resonance frequency and the quality factor of a DETF vary even between the two DETFs of a resonator.

Regarding the magnetic stack, we managed to adequately shift the hysteresis loop and obtain a constant magnetization equal to the saturation magnetization $M = M_S$ on the interval $[-1\text{mT}, 1\text{mT}]$ (Figure 6). This way, it is possible to guarantee the stability of the magnetization over the measurement scale. Concerning their deposition over the plate, it was done thanks to an RF sputtering

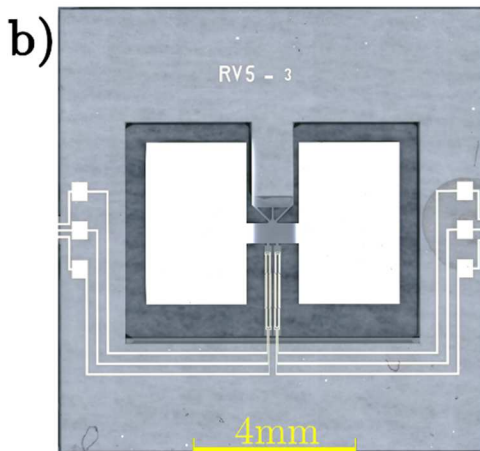
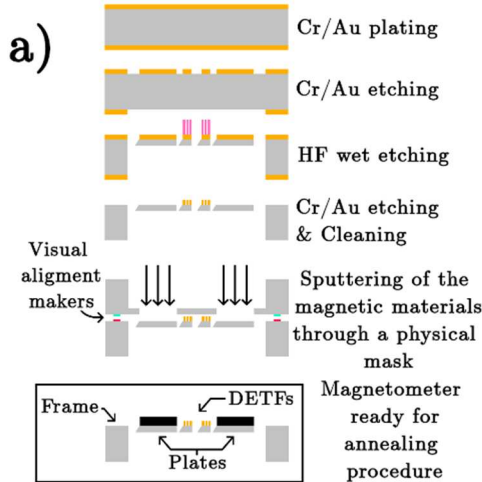


Figure 4. a) Fabrication process of a resonator b) Realisation of a resonator with magnetic materials on the plates

machine over a shadow mask which protects the DETFs with the electrodes, the frame and the pivot. .

Finally, to be able to measure a magnetic field with the magnetometer, it is compulsory to package it with a non-magnetic ceramic packaging and associate it with a proximity charge amplifier.

Measurements

To measure and track the resonance frequency of one DETF, it is possible to use a servo-loop on the phase of the electric signal coming from the electrodes, this is the role of the oscillator circuit. Therefore, an input electric signal is applied on the *drive* electrode, an output signal is retrieved on the *sense*, and the third electrode is connected to the mass. However, it will not be possible to measure a magnetic field without the help of a charge amplifier circuit. It is meant to amplify the electric signal coming from the sense electrode because of the low piezoelectric coupling factor of the quartz [14].

For K_B measurement, we used a magnetometer at atmospheric pressure linked to an amplifier circuit on a chip and an HF2LI with the Phase-Locked-Loop (PLL) for the oscillator circuit. The applied a magnetic field had an intensity of $B = 0.7\text{ mT}$ and was along one direction

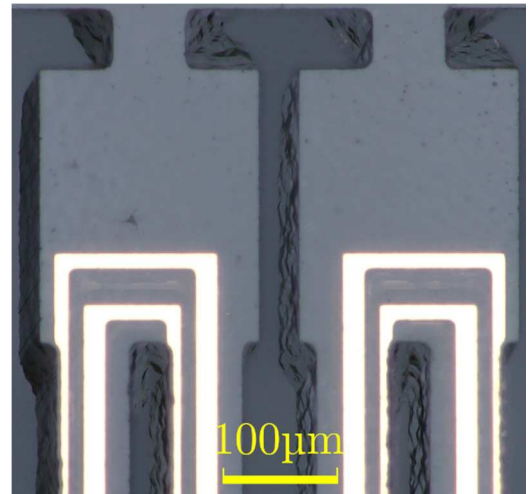


Figure 5. Side-walls around the top heads of the DETFS

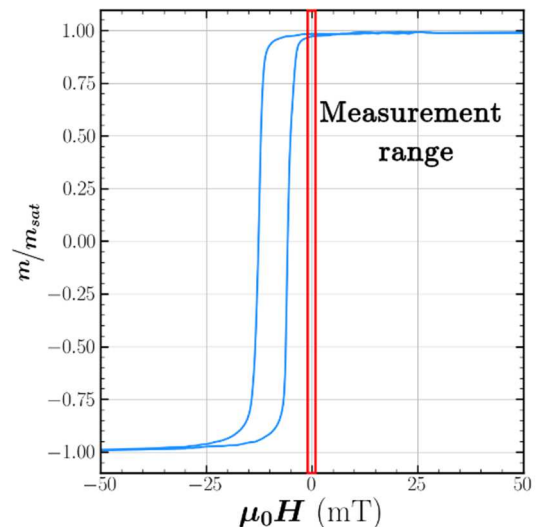


Figure 6. Hysteresis loop of the NiMn/CoFe stack

thanks to an Helmholtz coil. For the first DETF, we observed a shift of resonance frequency of $\Delta f_1 = 0.39$ Hz and for the second DETF, $\Delta f_2 = -0.66$ Hz. Therefore, the working principle is proven to be correct and the sensitivity is equal to $K_B = 1500$ Hz/T.

Secondly, for the measurement of the resonance frequency and the quality factor, we were able to measure under vacuum with an impedance-meter the characteristics of the Butterworth-van-Dyke RLC $\parallel C_0$ equivalent circuit of the resonating DETFs. We obtained $f_R = 122$ kHz with a quality factor of $Q = 29000$. Finally, thanks to previous works in the ONERA lab [7], it was possible to evaluate the detection limit $\sigma = 7.3$ nT (Table 1).

We can observe that the experimental measurements are close to the simulation results. The differences are due to the size and shapes of the side-walls that are not perfectly reproducible in the simulations.

	Simulation	Experimental
f_R (kHz)	132	122
Q (-)	45000	29000
K_B (Hz/T)	1040	1500
σ (nT)	6.8	7.3 (estimated)

Table 1. Comparison of simulation results and experimental measurements

CONCLUSION

We managed to conceive a new type of magnetometer thanks to finite element software and an analytical model, fabricate it in a clean room with a wet chemical etching process. We proved the working principle of the magnetometer to be in alignment with numerical simulations. Indeed, the characteristics f_R , Q , K_B and σ were measured or estimated and are within the scope of the current study.

We soon expect to verify experimentally the detection limit with a vacuumed packaging and use an FPGA for the oscillator circuit in order to have a fully embedded magnetometer.

ACKNOWLEDGEMENTS

This study is part of a PhD thesis under funding from AID/DGA (Defense Innovation Agency - French MoD) and was supported by the French ANR program Astrid Maturation (ANR-19-ASMA-0002-01). The authors would like to thank AID/DGA for their support.

REFERENCES

[1] E. Dorveaux, "Navigation Magnéto-Inertielle Principes et application à un système podométrique indoor," Mines ParisTech, 2012.

[2] J. Kynnäräinen *et al.*, "A 3D micromechanical compass," *Sensors Actuators, A Phys.*, vol. 142, no. 2, pp. 561–568, 2008.

[3] A. Herrera-May, J. Soler-Balcazar, H. Vázquez-

Leal, J. Martínez-Castillo, M. Viguera-Zuñiga, and L. Aguilera-Cortés, "Recent Advances of MEMS Resonators for Lorentz Force Based Magnetic Field Sensors: Design, Applications and Challenges," *Sensors*, vol. 16, no. 9, p. 1359, Aug. 2016.

- [4] L. Bian *et al.*, "A Resonant Magnetic Field Sensor with High Quality Factor Based on Quartz Crystal Resonator and Magnetostrictive Stress Coupling," *IEEE Trans. Electron Devices*, vol. 65, no. 6, pp. 2585–2591, 2018.
- [5] D. Ettelt, P. Rey, G. Jourdan, A. Walther, P. Robert, and J. Delamare, "3D magnetic field sensor concept for use in inertial measurement units (IMUs)," *J. Microelectromechanical Syst.*, vol. 23, no. 2, pp. 324–333, 2014.
- [6] P. Rangsten, C. Hedlund, I. V. Katardjiev, and Y. Bäcklund, "Etch rates of crystallographic planes in Z-cut quartz - Experiments and simulation," *J. Micromechanics Microengineering*, vol. 8, no. 1, pp. 1–6, 1998.
- [7] R. Levy and V. Gaudineau, "Phase noise analysis and performance of the Vibrating Beam Accelerometer," *2010 IEEE Int. Freq. Control Symp. FCS 2010*, pp. 511–514, 2010.
- [8] O. Le Traon, D. Janiaud, B. Lecorre, M. Pernice, S. Muller, and J. Y. Tridera, "Monolithic differential vibrating beam accelerometer within an isolating system between the two resonators," *Proc. IEEE Sensors*, vol. 2005, pp. 648–651, 2005.
- [9] M. Zhang, G. Luiz, S. Shah, G. Wiederhecker, and M. Lipson, "Eliminating anchor loss in optomechanical resonators using elastic wave interference," *Appl. Phys. Lett.*, vol. 105, no. 5, 2014.
- [10] J. Rodriguez *et al.*, "Direct Detection of Anchor Damping in MEMS Tuning Fork Resonators," *J. Microelectromechanical Syst.*, vol. 27, no. 5, pp. 800–809, 2018.
- [11] R. Lifshitz and M. Roukes, "Thermoelastic damping in micro- and nanomechanical systems," *Phys. Rev. B - Condens. Matter Mater. Phys.*, vol. 61, no. 8, pp. 5600–5609, 2000.
- [12] J. Nogués *et al.*, "Exchange bias in nanostructures," *Phys. Rep.*, vol. 422, no. 3, pp. 65–117, 2005.
- [13] C. Mauc, T. Perrier, J. Moulin, and P. Kayser, "Induced exchange bias in NiMn/CoFe multilayer thin films sputtered on a quartz substrate by field cooling," *J. Magn. Magn. Mater.*, vol. 544, no. September 2021, p. 168649, Feb. 2022.
- [14] R. Abdolvand, H. Fatemi, and S. Moradian, "Quality Factor and Coupling in Piezoelectric MEMS Resonators," H. Bhugra and G. Piazza, Eds. Cham: Springer International Publishing, 2017, pp. 133–152.